https://dx.doi.org/10.21577/0103-5053.20230054

J. Braz. Chem. Soc., Vol. 34, No. 10, 1420-1431, 2023

Article

Mitochondria-Targeted Ergosterol Peroxide Derivatives: Synthesis, Anticancer Properties and Their Preliminary Mechanism of Inhibiting MCF-7 Cell Proliferation

Wenkang Ren,[a] Jiale Wu,[a] Jiafeng Wang,[b] Haijun Wang,[a] Yinglong Han,[a] Yu Lin[,a] and Ming Bu*[,a]*

[a]*College of Pharmacy, Qiqihar Medical University, 161006 Qiqihar, China*

[b]*College of Pathology, Qiqihar Medical University, 161006 Qiqihar, China*

Ergosterol peroxide (EP) has been extensively studied for its antitumor activities. However, its further development has been restricted due to its limited intracellular accumulation and poor aqueous solubility. In this study, a novel triphenylphosphonium cation (TPP^+) moiety was coupled to ergosterol peroxide to precisely target it at tumor cell mitochondria. The synthesized Mito-EP derivatives Mito-EP-**3a-3d** displayed stronger cytotoxicity than the EP parent and exhibited selectively cytotoxic effects between cancer cells and normal gastric epithelial (GES-1) cells. The most potent compound, Mito-EP-**3b**, was 9.7-fold more efficacious than ergosterol peroxide in the MCF-7 (breast cancer) cell line and showed good selectivity (SI = IC_{50}GES-1/IC_{50}MCF-7 = 4.04, IC_{50}: concentrations to inhibit 50% of cell growth). Furthermore, Mito-EP-**3b** was able to decrease the mitochondrial membrane potential and induced reactive oxygen species production, accompanied by activating the expression of cytochrome c and Bax, while Bcl-2 expression was suppressed. The molecular mechanism may refer to the mitochondrial apoptotic pathway. Overall, the above results incentivize the further study of Mito-EP-**3b** derivatives as potent anticancer agents.

Keywords: triphenylphosphonium, ergosterol peroxide, anticancer activity, apoptosis, MCF-7

Introduction

Cancer is caused by malignant cell proliferation and is recognized worldwide as a disease with a high mortality rate.[1-3] Chemotherapy is still one of the most effective methods of cancer treatment today, but adverse side effects limit the clinical use of many drugs.[4] Therefore, it is an important task to develop new antitumor drugs with low toxicity and high efficiency. Natural products have a long history of medicinal use and are one of the main sources of anticancer drugs. In the 1950s, natural product camptothecin was isolated from *Camptotheca acuminata*, and further obtained the anticancer drugs Irinotecan and Topotecan through the structural modification of camptothecin.[5] Since then, there has been an international boom in the discovery and development of antitumor drugs from natural products. Among the 185 small molecule anticancer drugs marketed in the past 40 years, 120 are directly or indirectly derived from natural products, accounting for 65% of the total.[6] In summary, the discovery and structural modification of natural lead compounds is an important field of natural drug research and is one of the important directions for the development of new anticancer drugs with high efficiency and low toxicity.

Endoperoxides are a class of compounds with peroxy-bridged structures (–O–O–) that are abundant and biologically diverse in nature, and many endoperoxide natural products have been shown to have significant antitumor activities and potential medicinal value.[7] Artemisinin (**I**), gracilioether A (**II**), schinalactone A (**III**), talaperoxide B (**IV**) and other natural peroxides have been verified to have significant anticancer activities.[8-11] Dihydroartemisinin (**V**), a semi-synthesis product from artemisinin, has been shown to promote the degradation of platelet-derived growth factor receptor-α (PDGFRα) protein by targeting it and thus can selectively inhibit the proliferation of PDGFRα-positive ovarian cancer cells.[12] Not limited to natural products, many synthetic endoperoxides have also shown potential for development as clinical antitumor agents. Ishar and co-workers[13] reported the synthesis of a series of β-viologenone endoperoxides, among them, compound **3j** (**VI**) showed significant activities against A549 and MCF-7 cell lines, with concentrations to inhibit 50% of cell growth (IC_{50})

*e-mail: buming@qmu.edu.cn; linyu7373@163.com
Editor handled this article: Brenno A. D. Neto

values ranging from 0.001 to 7.7 μM.[13] Schirmeister *et al.*[14] synthesized plakortic acid (**VII**) successfully, which showed the potent inhibition of sensitive leukemic CCRF-CEM cell lines with the IC_{50} value of 0.19 μM. Cabrera-Afonso *et al.*[15] synthesized an endoperoxide **5** (**VIII**), which exhibited potent antiproliferative activity against HepG2 (hepatoma), HeLa (cervical cancer) and MDA-MB-231 (breast cancer) cell lines with IC_{50} values lower than 0.1 μM.[15] The above representative compounds of natural and synthetic endoperoxides are shown in Figure 1. It is desirable that the novel structure of endoperoxide provide a research direction for the development of new pharmacophores or new drugs.

Ergosterol peroxide (EP, **1**), a steroid containing a peroxy-bridge structure extracted from *Ganoderma lucidum* in the early stage of our group,[16-18] has significant anticancer activity and cell selectivity. The structure of EP is shown in Figure 2. The peroxide bridge of EP is considered to be an important pharmacophore, and the cytotoxic effects of EP on a variety of cancer cells is significantly enhanced compared to ergosterol, which has no peroxide bridge structure.[19-24] Due to the fact that the amount of ergosterol peroxide isolated from fungi was too little, it was not sufficient to be used clinically. Hence, we developed an approach to synthesize ergosterol peroxide from ergosterol.[25] In our previous works,[26-29] we found certain endoperoxide steroid derivatives that were able to modulate the production of reactive oxygen species (ROS) in tumor cells and further show cytotoxic activity against tumor cells through ROS-mediated molecular damage, protein level imbalance and cell cycle arrest. Therefore, ergosterol peroxide could be a valuable lead compound for anticancer drug development.

One of the major challenges in developing anticancer agents is increasing their selectivity, as well as reducing severe toxic side effects for normal tissues.[30] It is well known that tumor cells are easily resistant to apoptosis and that mitochondria are closely related to apoptotic pathways.[31-33] Hence, a possible promising strategy is to target therapeutic drugs to the mitochondria of tumor cells in order to improve selectivity as well as reduce the toxicity profile. Furthermore, recent research has proven that the mitochondrial membrane potential (MMP) is different between normal cells and cancer cells, which provided further possibility for mitochondria-targeting strategies in new drug design.[34-36] We are able to achieve this strategy by targeting natural products at the mitochondrial matrix with delocalized lipophilic cations. Various lipophilic cations, including triphenylphosphonium cation (TPP^+), rhodamine, cyanine cations, and cationic peptides, can be attached to the bioactive compound and selectively accumulate in the mitochondria of cancer cells based on the increased MMP of cancer cells compared with that of normal cells.[37-39] Among them, TPP^+ is the most successfully studied lipophilic cations, and many successful examples, including botulin,[40] betulin acid,[41] chlorambucil,[42] ursolic acid,[43] gallic acid[44] and artemisinin[45-47] have been reported to be designed as TPP^+ derivatives with improved antitumor effect and selectivity. The advantages of TPP^+ group are very prominent, such as the stability of the structure in biological systems, a combination of lipophilic and hydrophilic properties, the relatively simple synthesis and purification. Most importantly, TPP^+ was shown to be relatively safe in humans, thereby enhancing the potential clinical and translational significance of this class of molecules.[48] However, linking ergosterol peroxide with TPP^+ to obtain mitochondria-targeted ergosterol peroxide derivatives is not yet reported. Herein we reported the design, synthesis, and biological characterization of a series of novel derivatives of EP. Mito-EP-**3a-3d** were obtained by introducing a TPP^+ moiety into the 3-OH group of EP to improve their ability of targeting mitochondria of cancer

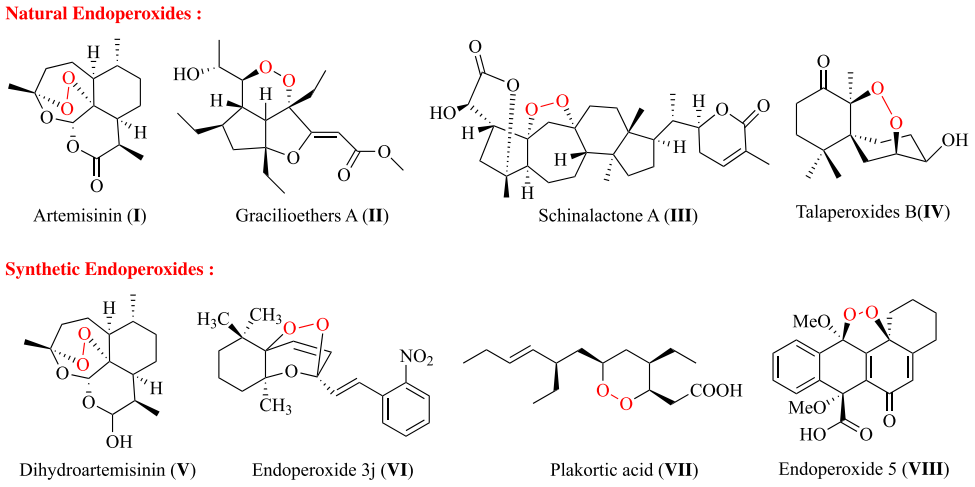

Figure 1. Some representative compounds of natural and synthetic endoperoxides.

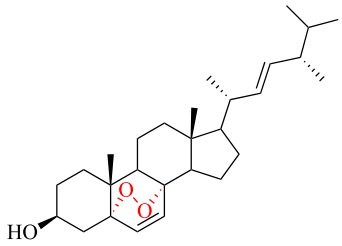

Figure 2. Structure of ergosterol peroxide (EP, **1**).

cells. Additionally, studies have found that the length of alkyl chains between TPP^+ and natural lead compounds may also affect the antitumor activity of TPP^+-based betulin acid, oleanolic acid, triptolide and others.[47-50] The length of the alkyl chain is an important factor for the performance of end products. Therefore, we also explored the effect of alkyl chain length on the activity of these derivatives. In addition, we also investigated the mechanism of the active compound by studying the relevant proteins involved in the mitochondrial apoptotic pathway.

Experimental

Chemistry

All chemicals and solvents were purchased from Zesheng-Chemical (Anhui, China). All reactions were monitored by thin-layer chromatography silica gel plates (Yinlong, Qingdao, China). The compounds were separated and purified by column chromatography using silica gel (300-400 mesh, Yinlong, Qingdao, China). The melting points of the pure solid compounds were carried out by a Haineng MP120 melting point apparatus (Fujian, China). The nuclear magnetic resonance (NMR) spectra were recorded on a AVANCE NEO 600 spectrometer (Bruker, Berlin, Germany). The low-resolution mass spectra of all intermediates were recorded on a Bruker Esquire 6000 mass spectrometer (Bruker, Germany). The high-resolution mass spectra data were obtained using a UPLC G2-XS Q-TOF (Waters, USA) and a TripleTOF 4600 (AB SCIEX, USA) with the electrospray ionization (ESI) source in a positive ion mode.

General procedure for the synthesis of intermediates EP-S-**1-4**

Ergosterol peroxide (**1**, 1 mmol), 3-bromopropionic acid, 4-bromobutyric acid, 5-bromovaleric acid or 6-bromonhexanoic acid (1.5 mmol) and dichloromethane (15 mL) were sequentially added into a 50 mL bottom flask, with 1-(3-dimethylaminopropyl)-3-ethylcarbodiimide hydrochloride (EDCI, 1.5 mmol) and 4-dimethylaminopyridine (DMAP, 0.2 mmol) added as catalysts. The mixture was kept at room temperature with stirring for 4-6 h, until the ergosterol peroxide disappeared completely. After the reaction, the organic solvent was evaporated through rotary evaporation, and then the intermediates EP-S-**1-4** were obtained by flash column chromatography.

5α,8α-Epidioxiergosta-6,22-dien-3β-yl 3-bromopropanoate (EP-S-**1**)

White solid; 64%; ^{1}H NMR (600 MHz, $CDCl_3$) δ 6.51 (d, 1H, *J* 8.4 Hz, C7-H), 6.23 (d, 1H, *J* 8.4 Hz, C6-H), 5.22 (dd, 1H, *J* 15.2, 7.7 Hz, C23-H), 5.14 (dd, 1H, *J* 15.2, 8.3 Hz, C23-H), 5.00 (m, 1H, C3-H), 3.41 (t, 2H, *J* 6.6 Hz, C3'-CH_2), 2.30 (t, 2H, *J* 7.3 Hz, C2'-CH_2), 2.12 (dd, 1H, *J* 14.6, 4.3 Hz), 2.04-1.99 (m, 3H), 1.90-1.87 (m, 2H), 1.84 (s, 1H), 1.77 (d, 2H, *J* 7.6 Hz), 1.70 (d, 1H, *J* 13.6 Hz), 1.58 (d, 2H, *J* 11.2 Hz), 1.51 (d, 2H, *J* 6.7 Hz), 1.47 (d, 1H, *J* 6.5 Hz), 1.37 (d, 1H, *J* 9.6 Hz), 1.25 (d, 2H, *J* 6.5 Hz), 1.23 (d, 2H, *J* 4.4 Hz), 1.00 (d, 3H, *J* 6.6 Hz, C18-H), 0.92-0.89 (m, 6H, C28-H, C21-H), 0.84-0.80 (m, 9H, C-19H, C26-H, C27-H); ^{13}C NMR (150 MHz, $CDCl_3$) δ 172.2 (C1'), 135.2 (C22), 135.1 (C6), 132.3 (C23), 130.9 (C7), 81.7 (C5), 79.4 (C8), 69.5 (C3), 56.2 (C17), 51.6 (C14), 51.0 (C9), 44.6 (C13), 42.8 (C24), 39.7 (C12), 39.3 (C20), 37.0 (C10), 34.3 (C4), 33.5 (C2'), 33.1 (C5), 32.0 (C1), 28.6 (C2, C3'), 26.3 (C16), 23.5 (C15), 20.9 (C11), 20.6 (C21), 20.0 (C26), 19.6 (C27), 18.1 (C19), 17.6 (C28), 12.9 (C18); MS (ESI) *m/z*, $[M + H]^+$ 563.3.

5α,8α-Epidioxiergosta-6,22-dien-3β-yl 4-bromobutyrate (EP-S-**2**)

White solid; 84%; ^{1}H NMR (600 MHz, $CDCl_3$) δ 6.44 (d, 1H, *J* 8.5 Hz, C7-H), 6.16 (d, 1H, *J* 8.5 Hz, C6-H), 5.15 (dd, 1H, *J* 15.3, 7.6 Hz, C23-H), 5.08 (dd, 1H, *J* 15.2, 8.4 Hz, C22-H), 4.97 (m, 1H, C3-H), 3.39 (t, 2H, *J* 6.4 Hz, C4'-CH_2), 2.39 (t, 2H, *J* 7.2 Hz, C2'-CH_2), 2.11 (m, 2H, C3'-CH_2), 2.05 (d, 1H, *J* 3.5 Hz), 1.95 (s, 2H), 1.88 (d, 2H, *J* 8.8 Hz), 1.78 (m, 1H, *J* 6.8 Hz), 1.68 (d, 1H, *J* 9.6 Hz), 1.63 (d, 1H, *J* 13.6 Hz), 1.54-1.48 (m, 3H), 1.44 (d, 2H, *J* 8.3 Hz), 1.40 (m, 1H), 1.36 (m, 1H), 1.30 (d, 1H, *J* 9.8 Hz), 1.20-1.15 (m, 3H), 1.14 (d, 1H, *J* 9.0 Hz), 0.93 (d, 3H, *J* 6.7 Hz, C18-H), 0.84 (d, 6H, *J* 8.4 Hz, C28-H, C21-H), 0.77 (s, 3H, C-19H), 0.75 (d, 3H, *J* 3.1 Hz, C26-H), 0.74 (d, 3H, *J* 3.1 Hz, C27-H); ^{13}C NMR (150 MHz, $CDCl_3$) δ 170.6 (C1'), 134.2 (C22), 134.0 (C6), 131.3 (C23), 129.9 (C7), 80.7 (C5), 78.4 (C8), 68.7 (C3), 55.2 (C17), 50.6 (C14), 50.0 (C9), 43.5 (C13), 41.8 (C24), 38.7 (C12), 38.3 (C20), 35.9 (C10), 33.3 (C4), 32.2 (C4'), 32.0 (C25), 31.8 (C2'), 31.7 (C1), 27.6 (C3'), 26.7 (C2), 25.3 (C16), 22.4 (C15), 19.9 (C11), 19.6 (C21), 18.9 (C26), 18.6 (C27), 17.1 (C19), 16.6 (C28), 11.9 (C18); MS (ESI) *m/z*, $[M + H]^+$ 577.3.

5α,8α-Epidioxiergosta-6,22-dien-3β-yl 5-bromovalerate (EP-S-**3**)

White solid; 87%; ^{1}H NMR (600 MHz, $CDCl_3$) δ 6.51 (d, 1H, *J* 8.5 Hz, C7-H), 6.23 (d, 1H, *J* 8.5 Hz, C6-H), 5.22 (dd, 1H, *J* 15.3, 8.5 Hz, C23-H), 5.14 (dd, 1H, *J* 15.3, 8.5 Hz, C22-H), 5.00 (m, 1H, C3-H), 3.41 (t, 2H, *J* 6.6 Hz, C5'-CH_2), 2.30 (t, 2H, *J* 7.3 Hz, C2'-CH_2), 2.12 (d, 1H, *J* 11.8 Hz), 2.01 (s, 2H), 1.95 (d, 2H, *J* 9.0 Hz), 1.88 (d, 2H, *J* 8.2 Hz, C4'-CH_2), 1.85 (d, 1H, *J* 6.6 Hz), 1.77 (d, 2H, *J* 7.4 Hz, C3'-CH_2), 1.75 (s, 1H), 1.70 (d, 1H, *J* 13.6 Hz), 1.61-1.54 (m, 3H), 1.51 (d, 2H, *J* 7.1 Hz), 1.46 (s, 1H), 1.40 (s, 1H), 1.35 (d, 1H, *J* 10.3 Hz), 1.27-1.19 (m, 4H), 1.00 (d, 3H, *J* 6.6 Hz, C18-H), 0.91 (d, 6H, *J* 8.8 Hz, C28-H, C21-H), 0.84-0.81 (m, 9H, C-19H, C26-H, C27-H); ^{13}C NMR (150 MHz, $CDCl_3$) δ 172.2 (C1'), 135.2 (C22), 135.1 (C6), 132.3 (C23), 130.9 (C7), 81.7 (C5), 79.4 (C8), 69.5 (C3), 56.2 (C17), 51.6 (C14), 51.0 (C9), 44.6 (C13), 42.8 (C24), 39.7 (C12), 39.3 (C20), 37.0 (C10), 34.3 (C4), 33.5 (C5'), 33.2 (C2'), 33.1 (C25), 33.1 (C4'), 32.0 (C1), 28.6 (C2), 26.3 (C16), 23.5 (C15), 23.4 (C3'), 20.9 (C11), 20.6 (C21), 20.0 (C26), 19.6 (C27), 18.1 (C19), 17.6 (C28), 12.9 (C18); MS (ESI) *m/z*, $[M + H]^+$ 591.3.

5α,8α-Epidioxiergosta-6,22-dien-3β-yl 6-bromohexanoate (EP-S-**4**)

White solid; 85%; ^{1}H NMR (600 MHz, $CDCl_3$) δ 6.51 (d, 1H, *J* 8.5 Hz, C7-H), 6.23 (d, 1H, *J* 8.5 Hz, C6-H), 5.22 (dd, 1H, *J* 15.2, 7.7 Hz, C23-H), 5.14 (dd, 1H, *J* 15.3, 8.4 Hz, C22-H), 5.00 (m, 1H, C3-H), 3.40 (t, 2H, *J* 6.7 Hz, C6'-CH_2), 2.28 (t, 2H, *J* 7.4 Hz, C2'-CH_2), 2.12 (dd, 1H, *J* 13.6, 5.4 Hz), 2.01 (s, 2H), 1.94 (d, 2H, *J* 8.2 Hz), 1.87 (d, 2H, *J* 7.5 Hz), 1.85 (d, 2H, *J* 6.8 Hz, C5'-CH_2), 1.74 (s, 1H), 1.71 (s, 1H), 1.63 (d, 2H, *J* 7.8 Hz, C3'-CH_2), 1.60-1.55 (m, 3H), 1.51 (d, 2H, *J* 9.1 Hz), 1.47 (d, 2H, *J* 3.7 Hz, C4'-CH_2), 1.45 (s, 1H), 1.40 (s, 1H), 1.35 (d, 1H, *J* 10.3 Hz), 1.27-1.19 (m, 4H), 1.00 (d, 3H, *J* 6.6 Hz, C18-H), 0.90 (s, 3H, 6H, C28-H), 0.84-0.81 (m, 9H, 3H, C-19H, C26-H, C27-H); ^{13}C NMR (150 MHz, $CDCl_3$) δ 172.5 (C1'), 135.2 (C22), 135.2 (C6), 132.3 (C23), 130.9 (C7), 81.7 (C5), 79.4 (C8), 69.4 (C3), 56.2 (C17), 51.6 (C14), 51.0 (C9), 44.5 (C13), 42.8 (C24), 39.7 (C12), 39.3 (C20), 36.9 (C10), 34.3 (C4), 33.5 (C6'), 33.2 (C25), 33.0 (C2'), 32.4 (C5'), 28.6 (C1), 27.6 (C2), 26.3 (C16, C4'), 24.1 (C3'), 23.4 (C15), 20.9 (C11), 20.6 (C21), 19.9 (C26), 19.6 (C27), 18.1 (C19), 17.6 (C28), 12.9 (C18); MS (ESI) *m/z*, $[M + H]^+$ 605.3.

General procedure for the synthesis of Mito-EP-**3a-3d**

Intermediates EP-S-**1-4** (1 mmol), triphenylphosphine (10 mmol) and acetonitrile (25 mL) were added into a 100 mL round-bottom flask. The mixture was stirred under reflux and maintained for 48-72 h until intermediates EP-S-**1-4** disappeared completely. After the reaction, the solvent was evaporated and the precipitate was washed with ether (5 mL × 3) to give Mito-EP-**3a-3d** as a brownish powder.

5α,8α-Epidioxiergosta-6,22-dien-3β-yl 3-(triphenylphosphonio)-propanoate bromide (Mito-EP-**3a**)

Brownish powder; 70%; mp 130-133 °C; ^{1}H NMR (600 MHz, $CDCl_3$) δ 7.81 (dd, 6H, *J* 12.7, 7.7 Hz, Ar-H), 7.75 (t, 3H, *J* 8.5 Hz, Ar-H), 7.66 (td, 6H, *J* 7.7, 3.4 Hz, Ar-H), 6.46 (d, 1H, *J* 8.5 Hz, C7-H), 6.16 (d, 1H, *J* 8.5 Hz, C6-H), 5.20 (dd, 1H, *J* 15.2, 7.7 Hz, C23-H), 5.11 (dd, 1H, *J* 15.3, 8.4 Hz, C22-H), 4.53 (m, 1H, C3-H), 4.28 (s, 1H, C3'-H), 4.00 (s, 1H, C3'-H), 3.10 (s, 1H, C2'-H), 2.91 (s, 1H, C2'-H), 1.99 (s, 1H), 1.91 (s, 1H), 1.83 (s, 4H), 1.71 (s, 1H), 1.66 (s, 1H), 1.60 (d, 1H, *J* 13.4 Hz), 1.55 (s, 1H), 1.53 (s, 1H), 1.46 (s, 1H), 1.43 (s, 1H), 1.41 (s, 1H), 1.39 (s, 1H), 1.36 (s, 1H), 1.23 (m, 2H), 1.20 (s, 1H), 1.18 (s, 1H), 0.97 (s, 3H, C18-H), 0.88 s, (3H, C28-H), 0.80 (dd, 9H, *J* 6.3, 3.6 Hz, C21-H, C26-H, C27-H), 0.78 (d, 3H, *J* 3.5 Hz, C19-H); ^{13}C NMR (150 MHz, $CDCl_3$) δ 170.0 (C1'), 135.1 (Ar-4), 134.0 (Ar-3), 133.9 (C22), 132.4 (C6), 130.9 (C23), 130.6 (Ar-2), 130.5 (C7), 118.5 (Ar-1), 81.8 (C5), 79.6 (C8), 70.9 (C3), 56.3 (C17), 51.7 (C14), 51.1 (C9), 44.7 (C13), 42.9 (C24), 39.8 (C12), 39.3 (C20), 37.0 (C10), 34.2 (C4), 33.1 (C25, 2'), 29.8 (C1), 28.7 (C2), 26.0 (C16), 23.4 (C15), 20.9 (C3'), 20.7 (C11), 20.0 (C21), 19.7 (C26), 18.1 (C27), 17.7 (C19), 14.2 (C28), 12.9 (C18); HRMS (ESI) *m/z*, calcd. for $C_{49}H_{62}BrO_4P$ $[M + H]^+$: 825.3647, found: 825.3641.

5α,8α-Epidioxiergosta-6,22-dien-3β-yl 4-(triphenylphosphonio)-butyrate bromide (Mito-EP-**3b**)

Brownish powder; 82%; mp 139-143 °C; ^{1}H NMR (600 MHz, $CDCl_3$) δ 7.82 (dd, 6H, *J* 12.7, 7.7 Hz, Ar-H), 7.76-7.73 (m, 3H, Ar-H), 7.65 (td, 6H, *J* 7.6, 3.2 Hz, Ar-H), 6.46 (d, 1H, *J* 8.5 Hz, C7-H), 6.19 (d, 1H, *J* 8.5 Hz, C6-H), 5.18 (dd, 1H, *J* 15.2, 8.5 Hz, C23-H), 5.10 (dd, 1H, *J* 15.2, 8.5 Hz, C22-H), 4.92 (m, 1H, C3-H), 3.92 (s, 2H, C4'-H), 2.80 (s, 2H, C2'-H), 2.06 (d, 1H, *J* 13.8 Hz), 1.97 (d, 2H, *J* 12.0 Hz), 1.92 (d, 2H, *J* 10.2 Hz), 1.85 (d, 2H, *J* 10.9 Hz), 1.81 (d, 2H, *J* 6.8 Hz, C3'-H), 1.70 (d, 1H, *J* 9.2 Hz), 1.65 (d, 1H, *J* 13.7 Hz), 1.55 (s, 1H), 1.53 (s, 1H), 1.51 (s, 1H), 1.46 (s, 1H), 1.44 (s, 1H), 1.41 (s, 1H), 1.35 (s, 1H), 1.32 (s, 1H), 1.22 (s, 2H), 1.18 (d, 2H, *J* 3.7 Hz), 0.96 (d, 3H, *J* 6.6 Hz, C18-H), 0.87 (d, 3H, *J* 6.8 Hz, C28-H), 0.85 (s, 3H, C21-H), 0.80-0.77 (m, 9H, C-19H, C26-H, C27-H); ^{13}C NMR (150 MHz, $CDCl_3$) δ 171.3 (C1'), 134.0 (Ar-4), 132.8 (Ar-3), 132.7 (C22), 131.3 (C6), 129.8 (C23), 129.5 (Ar-2), 129.4 (C7), 117.5 (Ar-1), 80.8 (C5), 78.4 (C8),

68.8 (C3), 55.2 (C17), 50.6 (C14), 50.1 (C9), 43.6 (C13), 41.8 (C24), 38.7 (C12), 38.3 (C20), 35.9 (C10), 33.3 (C4), 32.0 (C2'), 28.7 (C25), 27.6 (C1), 25.2 (C2), 22.3 (C16), 21.6 (C15), 20.7 (C4'), 20.3 (C3'), 19.9 (C11), 19.6 (C21), 18.9 (C26), 18.6 (C27), 17.1 (C19), 16.6 (C28), 11.9 (C18); HRMS (ESI) *m/z*, calcd. for $C_{50}H_{64}BrO_4P$ $[M + H]^+$: 839.3804, found: 839.3800.

5α,8α-Epidioxiergosta-6,22-dien-3β-yl 5-(triphenylphosphonio)valerate bromide (Mito-EP-**3c**)

Brownish powder; 85%; mp 151-154 °C; ^{1}H NMR (600 MHz, $CDCl_3$) δ 7.81-7.79 (m, 6H, Ar-H), 7.71 (d, 6H, *J* 4.3 Hz, Ar-H), 7.65 (s, 1H, Ar-H), 7.56 (s, 1H, Ar-H), 7.48 (s, 1H, Ar-H), 6.50 (d, 1H, *J* 8.5 Hz, C7-H), 6.21 (d, 1H, *J* 8.5 Hz, C6-H), 5.23 (dd, 1H, *J* 15.2, 8.4 Hz, C23-H), 5.15 (dd, 1H, *J* 15.2, 8.4 Hz, C22-H), 4.87 (m, 1H, C3-H), 4.13 (t, 2H, *J* 7.1 Hz, C5'-CH_2), 2.36 (t, 2H, *J* 6.5 Hz, C2'-CH_2), 2.22 (d, 1H, *J* 7.1 Hz), 1.99 (d, 2H, *J* 8.1 Hz), 1.95 (d, 2H, *J* 6.2 Hz), 1.85 (d, 1H, *J* 6.6 Hz), 1.76 (s, 1H), 1.70 (d, 2H, *J* 7.8 Hz, C3'-CH_2), 1.68 (s, 1H), 1.57 (t, 3H, *J* 17.2 Hz), 1.50 (m, 2H), 1.46 (d, 1H, *J* 6.6 Hz), 1.40 (d, 1H, *J* 5.1 Hz), 1.37 (s, 1H), 1.27 (s, 1H), 1.25 (d, 3H, *J* 7.0 Hz), 1.23 (d, 2H, *J* 7.2 Hz, C4'-CH_2), 1.00 (d, 3H, *J* 6.6 Hz, C18-H), 0.91 (d, 3H, *J* 6.8 Hz, C28-H), 0.88 (s, 3H, C21-H), 0.83 (dd, 9H, *J* 8.5, 5.3 Hz, C-19H, C26-H, C27-H); ^{13}C NMR (150 MHz, $CDCl_3$) δ 172.4 (C1'), 135.1 (Ar-4), 133.7 (Ar-3), 132.3 (C22), 132.1 (C6), 130.8 (C23), 130.6 (Ar-2), 128.6 (C7), 118.6 (Ar-1), 81.8 (C5), 79.5 (C8), 69.4 (C3), 56.2 (C17), 51.6 (C14), 51.0 (C9), 44.6 (C13), 42.8 (C24), 39.7 (C12), 39.3 (C20), 36.9 (C10), 34.3 (C4), 33.4 (C2'), 33.1 (C25), 33.0 C1), 28.6 (C2), 26.2 (C16), 23.3 (C15), 22.3 (C5'), 21.7 (C4'), 21.4 (C3'), 20.9 (C11), 20.6 (C21), 19.9 (C26), 19.6 (C27), 18.1 (C19), 17.6 (C28), 12.9 (C18); HRMS (ESI) *m/z*, calcd. for $C_{51}H_{66}BrO_4P$ $[M + H]^+$: 853.3960, found: 853.3959.

5α,8α-Epidioxiergosta-6,22-dien-3β-yl 6-(triphenylphosphonio)hexanoate bromide (Mito-EP-**3d**)

Brownish powder; 81%; mp 135-138 °C; ^{1}H NMR (600 MHz, $CDCl_3$) δ 7.77 (d, 6H, *J* 12.7 Hz, Ar-H), 7.72 (s, 3H, Ar-H), 7.64 (s, 6H, Ar-H), 6.43 (d, 1H, *J* 8.5 Hz, C7-H), 6.16 (d, 1H, *J* 8.5 Hz, C6-H), 5.15 (dd, 1H, *J* 15.2, 8.5 Hz, C23-H), 5.07 (dd, 1H, *J* 15.2, 8.5 Hz, C22-H), 4.85 (m, 1H, C3-H), 3.77 (s, 2H, C6'-CH_2), 2.17 (s, 2H, C2'-CH_2), 1.98 (d, 1H, *J* 5.5 Hz), 1.94 (d, 2H, *J* 12.2 Hz), 1.89 (d, 2H, *J* 15.4 Hz), 1.80 (s, 1H), 1.78 (d, 2H, *J* 6.8 Hz, C3'-CH_2), 1.64 (m, 2H), 1.60 (s, 1H), 1.57 (s, 2H), 1.53-1.50 (s, 3H), 1.48 (d, 2H, *J* 6.6 Hz, C4'-CH_2), 1.42 (d, 2H, *J* 10.6 Hz), 1.39 (s, 1H), 1.30 (dd, 2H, *J* 19.1, 9.3 Hz), 1.18 (d, 2H, *J* 11.1 Hz, C5'-CH_2), 1.14 (d, 3H, *J* 6.3 Hz), 1.03 (s, 1H), 0.93 (d, 3H, *J* 6.5 Hz, C18-H), 0.85-0.82 (m, 6H, C28-H, C21-H), 0.77-0.74 (m, 9H, C-19H, C26-H, C27-H); ^{13}C NMR (150 MHz, $CDCl_3$) δ 171.8 (C1'), 134.2 (C22), 134.0 (Ar-4), 132.6 (Ar-3), 131.3 (C6), 129.8 (C23), 129.5 (Ar-2), 117.7 (C7), 117.1 (Ar-1), 80.8 (C5), 78.4 (C8), 68.3 (C3), 55.1 (C17), 50.6 (C14), 50.0(C9), 43.5 (C13), 41.7 (C24), 38.7 (C12), 38.3 (C20), 35.9 (C10), 33.3 (C4), 32.9 (C2'), 32.1 (C25), 32.0 (C1), 28.7 (C4'), 27.6 (C2), 25.2 (16), 23.3 (15), 22.3 (C6'), 21.9 (C5'), 21.5 (C3'), 19.8 (C11), 19.6 (C21), 18.9 (C26), 18.6 (C27), 17.1 (C19), 16.5 (C28), 11.8 (C18); HRMS (ESI) *m/z*, calcd. for $C_{52}H_{68}BrO_4P$ $[M + H]^+$: 867.4117, found: 867.4110.

Cells culture and MTT assays

HepG2 (hepatoma), MCF-7 (breast cancer), HeLa (cervical cancer) and human stomach normal cell line (GES-1) cells were obtained from the Cell Bank of Chinese Academy of Sciences (Shanghai, China). Cells were cultured in Roswell Park Memorial Institute (RPMI)-1640 medium (Corning, USA) supplemented with 10% fetal bovine serum (FBS, Gibco BRL, Grand Island, USA), 100 units mL^{-1} penicillin, and 100 μg mL^{-1} streptomycin (HyClone, Utah, USA) in a humidified atmosphere of 5% CO_2 at 37 °C. Cisplatin, ergosterol peroxide and its derivatives (stock solution of 40 mM in dimethyl sulfoxide (DMSO)) were stored at −20 °C. Before the experiment, the solutions were diluted with RPMI-1640 medium to obtain the working solutions of all the tested compounds. The final concentration of DMSO (in the working solution) was less than 0.1%. The cytotoxic activities of all compounds were evaluated by the 3-(4, 5-dimethylthiazolyl-2)-2, 5-diphenyltetrazolium bromide (MTT) method. The cells were cultured into 96-well plates (100 μL *per* well) at a concentration of 1×10^4 mL^{-1} for 24 h. Then, the cells were treated with gradient concentration of compounds (0, 1, 5, 10, 20, 40 μM) and cisplatin (0, 0.5, 1, 2, 4, 8 μM) for 48 h, then 10 μL MTT (Sigma Chemical Co., Ltd., USA) solution were added into each well for 4 h. The MTT was removed, and 100 μL DMSO (*per* well) were added to the plate, to dissolve the formazan crystals. The absorbance values were measured at 492 nm using microplate reader (Bio-Rad iMARK, USA). The IC_{50} was defined as the concentration of the compound that inhibited cell proliferation by 50%. IC_{50} values were calculated via SPSS Statistics 24.0[51] and expressed as mean ± standard deviation (SD).

Determination of morphological changes of cells

MCF-7 cells were seeded into 6-well plates at a concentration of 1×10^6 cells *per* well and cultured for

12 h. Following Mito-EP-**3b** treatment for 48 h, the tumor cells were double stained with a mixture of acridine orange/ethidium bromide (AO/EB) dyes buffer solution for 20 min. The AO/EB staining kit was obtained from Beyotime Biotechnology (Nanjing, China). The tumor cells were collected carefully and resuspended in phosphate buffer solution (PBS), and then the cell samples were studied and photographed under a fluorescence microscope (Obeserve. A1, Zeiss, Germany).

Apoptosis analysis by flow cytometry

Apoptosis was determined by staining cells with a BD 556547 Annexin V-FITC/PI detection kit (BD Biosciences, USA). Briefly, MCF-7 cells were seeded on six-well plates and incubated with compound Mito-EP-**3b** (0, 1, 2 and 4 μM) for 48 h. Cells were collected and washed twice with cold PBS and resuspended in 300 μL of 1 × binding buffer. 5 μL fluorescein 5-isothiocyanate (FITC)-conjugated annexin V were added and mixed gently. After incubation at room temperature for 15 min in the dark, 5 μL of propidium iodide (PI) was added and mixed gently. After incubation at room temperature for another 15 min in the dark, the samples were analyzed by a flow cytometry (BD, FACSCalibur, USA).

Analysis of mitochondrial membrane potential

MCF-7 cells treated with compound Mito-EP-**3b** or vehicle solvent for 48 h, washed with PBS and stained with JC-1 dye at 37 °C for 20 min according to the manufacturer's instructions (BD Biosciences, USA). Stained cells were washed three times with staining buffer and re-suspended in 300 μL of staining buffer. The percentage of cells with healthy or collapsed mitochondrial membrane potentials was monitored by flow cytometry analysis.

Measurement of ROS by flow cytometry

Intracellular ROS levels were examined using 2',7'-dichloro-fluorescein diacetate (DCFH-DA). MCF-7 cells were seeded in 12-well plates (1×10^6 cells *per* well) for 24 h and then treated with and cultured Mito-EP-**3b** (0, 1, 2 and 4 μM) for 48 h. After treatment, according to the manufacturer's instructions (Thermo Fisher Scientific, USA), 400 μL of 10 μM L^{-1} DCFH-DA was added to each well and incubated for 20 min. The stained cells were washed three times with serum-free culture medium and analyzed using a flow cytometer. The expression level of ROS is shown by fluorescence intensity.

Western blot analysis

MCF-7 cells were treated with varying concentrations of Mito-EP-**3b** for 48 h. Then, the MCF-7 cells were harvested and lysed in radioimmunoprecipitation (RIPA) buffer and boiled for 10 min at 100 °C. Equal amounts of proteins (30 μg) were separated on a 10% sodium dodecyl sulphate-polyacrylamide gel electrophoresis (SDS-PAGE) gel and transferred to nitrocellulose membranes. The membranes were blocked with 5% BSA and probed with a 1:1000 dilution of primary polyclonal antibody against Cl-caspase-9 and Cl-caspase-7 (Cell Singaling Technology, Inc., Boston, USA), glyceraldehyde-3-phosphate dehydrogenase (GAPDH) (Cell Singaling Technology, Boston, USA), Bcl-2 (Santa Cruz Biotechnology, Inc., Santa Cruz, USA), Bax (Proteintech Group, Inc., Chicago, USA), cytochrome c (Proteintech Group, Inc., Chicago, USA). Then, the membranes were incubated with a 1:5000 dilution of horseradish peroxidase-conjugated secondary antibody for 2 h. The blots were detected using enhanced chemiluminescence reagent with a fully automatic gel imaging system (ChemiDoc™ MP, Bio-Rad, Singapore, Republic of Singapore). The relative expression was calculated by normalizing the expression of the control group to 1 for comparison.

Data and statistical analysis

All data analysis and image processing were visualized using IBM SPSS Statistics 24.0 (SPSS Inc., Chicago, IL, USA).[51] Comparisons were performed by one-way analysis of variance (ANOVA), and $P < 0.05$ was considered a statistically significant difference.

Results and Discussion

Chemistry

The synthesis route for the new Mito-EP derivatives is depicted in Scheme 1. The ergosterol peroxide (**1**) was prepared from ergosterol according to a previously described method.[24] Intermediates EP-S-**1-4** were synthesized by the esterification of EP, and the corresponding acid used EDCI and DMAP as coupling agents in dichloromethane. The target Mito-EP derivatives, Mito-EP-**3a-3d**, were obtained by reacting with intermediates EP-S-**1-4**, respectively, with triphenylphosphine in refluxing condition.

In vitro cytotoxic effects of Mito-EP-**3a-3d**

After chemical synthesis, the cytotoxic effects of these

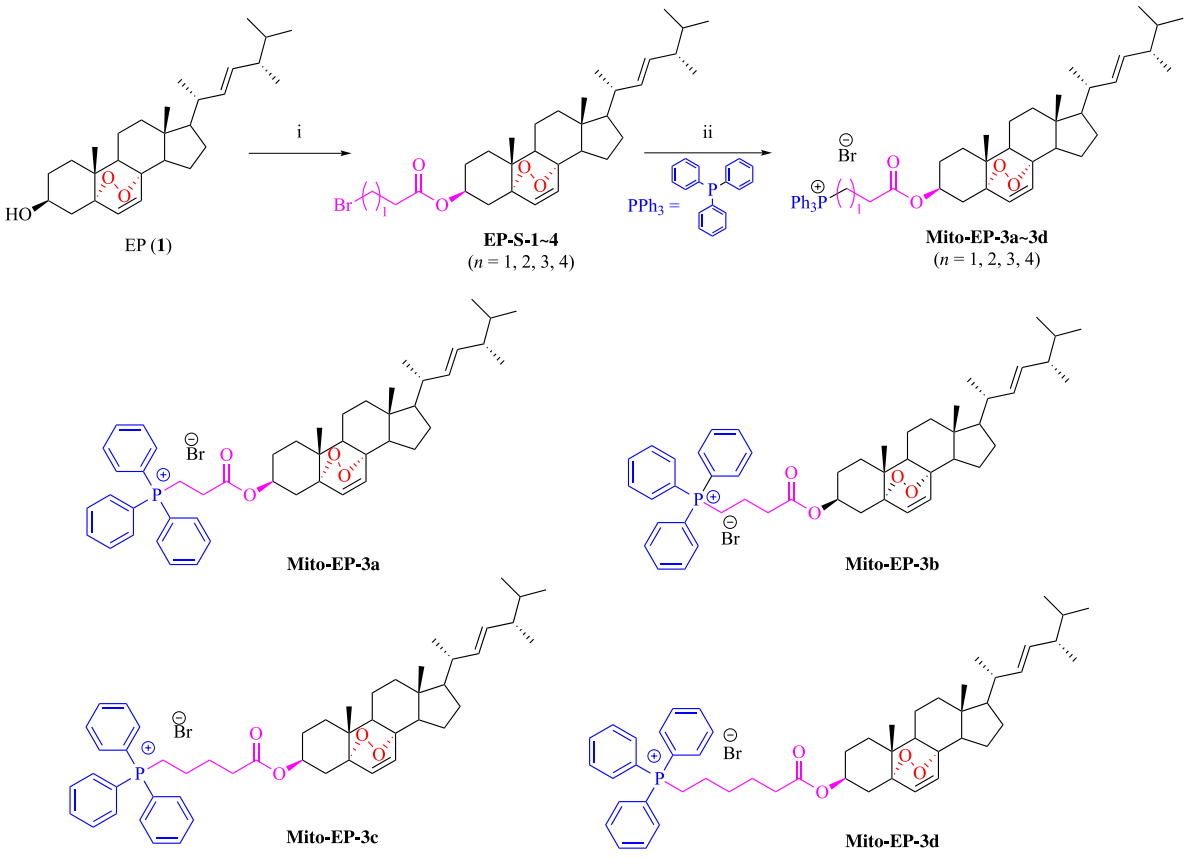

Scheme 1. Synthesis of mitochondria-targeted ergosterol peroxide derivatives **Mito-EP-3a-3d**. Reagents and conditions: (*i*) appropriate substituent (3-bromopropionic acid, 4-bromobutyric acid, 5-bromovaleric acid or 6-bromonhexanoic acid), DMAP, EDCI, dry dichloromethane, rt, 4-6 h, 64-87%; (*ii*) triphenylphosphine, acetonitrile, reflux, 24-48 h, 70-85%.

ergosterol peroxide Mito-derivatives on human cancer cells HepG2 (hepatoma), MCF-7 (breast cancer) and HeLa (cervical cancer) were evaluated using MTT assay. Ergosterol peroxide and cisplatin (DDP) were used as positive controls. A human stomach normal cell line (GES-1) was used to compare the selectivity of the derivatives. As shown in Table 1, the EP derivatives Mito-EP-**3a-3d** exhibited improved cytotoxic potency compared to the parent compound ergosterol peroxide against all three human tumor cell lines, proving that it is worth modifying the C-3 OH group of ergosterol peroxides with TPP.

To preclude the possibility that the cytotoxicity of new derivatives could stem from the TPP moiety, TPP was included as control. As shown in Table 1, no obvious cytotoxicity was found for TPP in any kind of tested cell lines, thus confirming the vital role of the new derivative as a whole structure. Although the Mito-EP-**3a-3d** exhibited increased cytotoxic effects toward GES-1 cells compared to

Table 1. Cytotoxic effects of the Mito-EP-derivatives **3a-3d**

Compound	IC_{50}[a] / μM				
	HepG2	MCF-7	HeLa	GES-1	SI[b]
TPP	> 100	> 100	> 100	> 100	–
Mito-EP-**3a**	2.11 ± 0.23	2.27 ± 0.08	4.98 ± 0.38	8.87 ± 0.65	3.90
Mito-EP-**3b**	2.34 ± 0.42	2.04 ± 0.10	4.65 ± 0.47	8.26 ± 0.58	4.04
Mito-EP-**3c**	4.40 ± 0.38	3.33 ± 0.27	6.33 ± 0.65	12.34 ± 1.02	3.70
Mito-EP-**3d**	9.34 ± 1.24	6.87 ± 0.82	8.74 ± 0.76	17.28 ± 1.13	2.51
EP (**1**)	18.36 ± 0.96	19.80 ± 1.50	23.24 ± 1.63	48.74 ± 1.95	2.46
Cisplatin	5.27 ± 0.27	4.05 ± 0.88	4.97 ± 0.64	–	–

[a]IC_{50}: concentration to inhibit 50% of cell growth, which is measured by the MTT assay. The value is expressed as mean ± SD of three independent experiments; [b]SI: IC_{50} for GES-1 cell line/IC_{50} for MCF-7 cell line. –: not determined. HepG2: hepatoma; MCF-7: breast cancer; HeLa: cervical cancer; GES-1: human stomach normal cell line; TPP: triphenylphosphonium; EP: ergosterol peroxide.

ergosterol peroxide parent, comparisons of the IC_{50} values between three tumor cells (HepG2, MCF-7, HeLa) and GES-1 cells demonstrated that Mito-EP-**3a-3d** are more cytotoxic to tumor cells than GES-1 cells, exhibiting certain selectivity towards tumor cells.

Among all three tested tumor cell lines, the MCF-7 and HepG2 cell lines were relatively more sensitive to the lethal effects of these derivatives. In the HepG2 cell line, all four compounds (Mito-EP-**3a**-**3d**) showed significant cytotoxic effects with IC_{50} ranging from 2.11 to 9.34 μM. In MCF-7 cell lines, all four compounds exhibited significant cytotoxicity with IC_{50} ranging from 2.04 to 6.87 μM. In the HeLa cell line, all four compounds also exhibited remarkable cytotoxicity with IC_{50} values ranging from 4.65 to 8.74 μM. Among all four derivatives, compounds Mito-EP-**3a**, Mito-EP-**3b** and Mito-EP-**3c** showed higher activity than cisplatin against all three cancer cell lines. In addition, Mito-EP-**3a** and Mito-EP-**3b** showed similar cytotoxicity to MCF-7 and HepG2 cell lines. Mito-EP-**3b** had an 9.70-fold higher activity than ergosterol peroxide in MCF-7 cell line and showed good selectivity (SI = IC_{50}GES-1/IC_{50}MCF-7 = 4.04) against ergosterol peroxide (SI = IC_{50}GES-1/IC_{50}MCF-7 = 2.46). A structure-activity relationship (SAR) analysis proved that the length of the carbon chain could affect the cytotoxic effects of all these derivatives. The antitumor activities of Mito-EP-**3a** and MitoEP-**3b** were superior to that of Mito-EP-**3c** or Mito-EP-**3d**, indicating that the length of linker had a significant effect on the antitumor activities of these compounds. Thus, Mito-EP-**3b**, with the highest efficacy and high selectivity against MCF-7 cells, was selected for the following cellular mechanism studies in MCF-7 cells.

Mito-EP-**3b** promoted apoptosis in MCF-7 cells

To assess whether the Mito-EP-**3b** was able to promote the apoptosis in MCF-7 cells, the apoptosis-associated cellular morphological changes were detected by the acridine orange/ethidium bromide (AO/EB) double-staining method. After being treated with different concentrations of Mito-EP-**3b** (0, 1, 2 and 4 μM) for 48 h, the AO/EB double staining method was used to detect the cellular morphological changes. As shown in Figure 3, MCF-7 cells generated obvious bright red nuclear vesicles, nuclear roundness and nuclear shrinkage in a dose-dependent manner. The morphology of untreated cells was almost intact and stained bright green. In addition, in order to quantify the percentage of apoptosis in MCF-7 cells induced by Mito-EP-**3b**, the annexin V and propidium iodide (AV/PI) double staining was carried out. As shown in Figure 4, after treatment with Mito-EP-**3b** at the concentration of 1, 2 and 4 μM for 48 h,

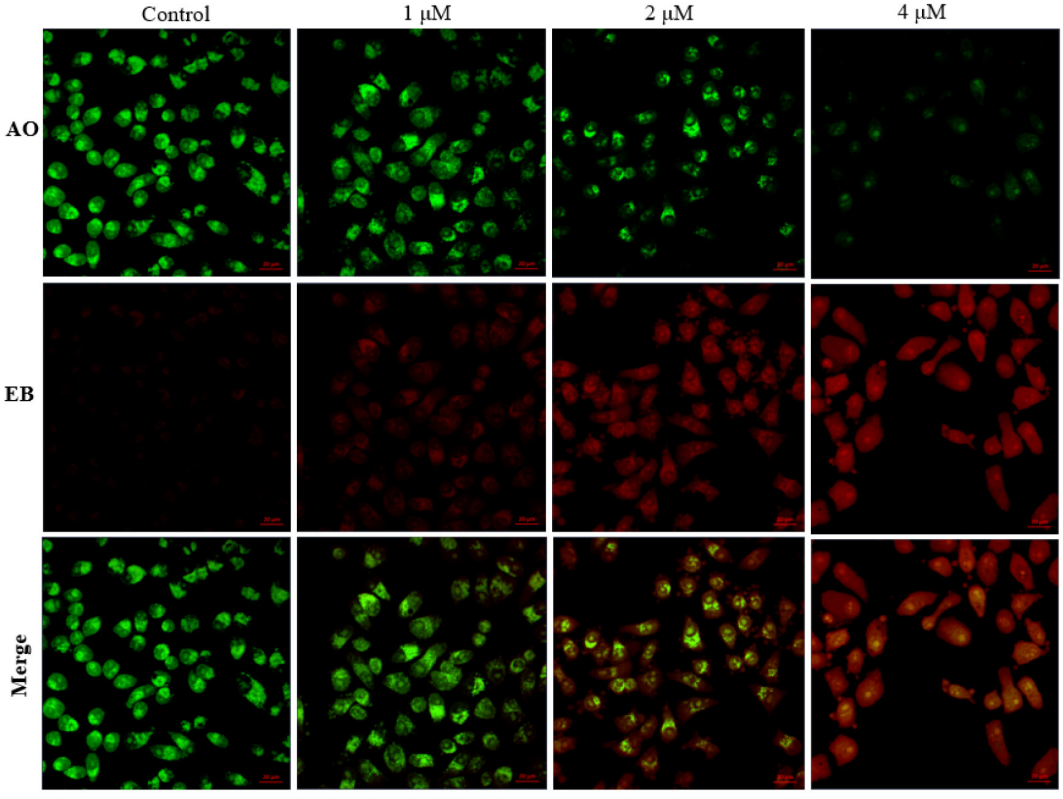

Figure 3. The effect of **Mito-EP-3b** on the cellular morphological changes of MCF-7 cells was determined by the AO/EB method.

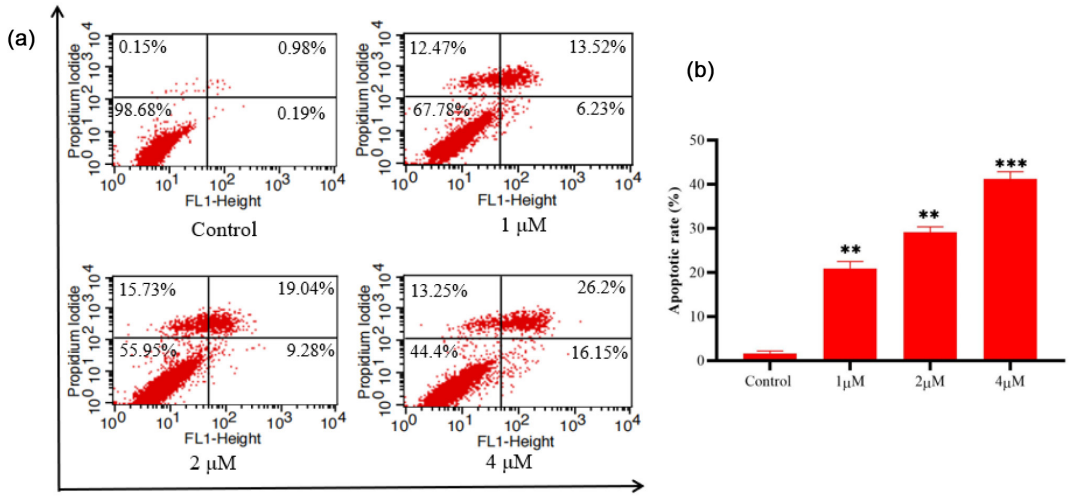

Figure 4. Detection of apoptosis using the annexin V-FITC/PI staining of Mito-EP-**3b** on MCF-7 cells. (a) MCF-7 cells were treated with Mito-EP-**3b** and then detected apoptosis using annexin V-FITC/PI assay by flow cytometry. (b) Quantitative analysis of apoptotic cells after treatment with Mito-EP-**3b**. Data are represented as average ± SD (n = 3). $^{**}P < 0.01$, $^{***}P < 0.001$.

the percentage of apoptosis cells markedly increased from 19.75 to 42.35% in a dose-dependent manner, while the control group was only 1.17%.

Mito-EP-**3b** decreased the MMP ($\Delta\psi_m$) of MCF-7 cells

It is well known that loss of mitochondrial membrane potential (MMP, $\Delta\psi_m$) is an important sign of the earliest events in the tumor cells apoptosis cascade. Since the new analogs were designed to target the mitochondria, we, therefore, decided to examine the influence of Mito-EP-**3b** on the $\Delta\psi_m$ of MCF-7 cells with the JC-1 staining method. As shown in Figure 5, MCF-7 cells were treated with different concentrations of Mito-EP-**3b** (0, 1, 2 and 4 μM) for 48 h and the percentage of low MMP cells increased correspondingly from 3.50 to 33.48% in a dose-dependent manner, which proved that Mito-EP-**3b** led to the collapse of MMP and then induced tumor cell apoptosis.

Mito-EP-**3b** induced the production of ROS in MCF-7 cells

Mitochondria are the main organelle that produces ROS, and ROS has been indicated to have a double sword role in the cytotoxicity in cancer cells. Therefore, in the sequence, we evaluated how the treatment with Mito-EP-**3b** in MCF-7 cells impacts the production of ROS by flow cytometry analysis. We used probe DCFH-DA to monitor intracellular ROS levels after being treated with Mito-EP-**3b**. MCF-7 cells were treated with Mito-EP-**3b** (0, 1, 2 and 4 μM) for 48 h, and then analyzed by flow cytometry. As shown in Figure 6, we found that Mito-EP-**3b** induced ROS generation significantly. Mito-EP-**3b** was able to increase

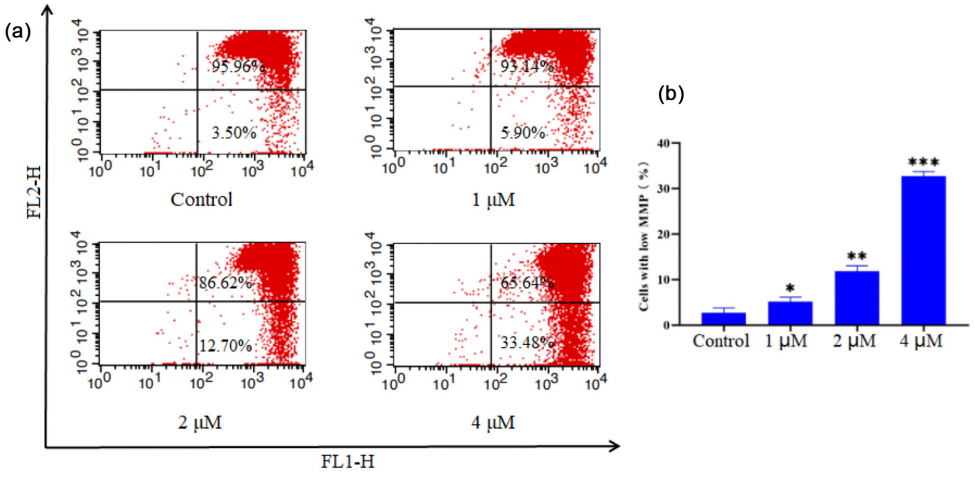

Figure 5. The effect of Mito-EP-**3b** on MMP in MCF-7 cells was determined by flow cytometry. (a) MCF-7 cells were treated with Mito-EP-**3b** and then detected by flow cytometry after JC-1 dye staining. (b) Quantitative analysis of the ratio of JC-1 monomers after treatment with different concentrations of Mito-EP-**3b**. Data are represented as average ± SD (n = 3). $^{*}P < 0.05$, $^{**}P < 0.01$, $^{***}P < 0.001$.

the intracellular ROS level at 4 μM by about 18.56% compared to the control group.

Mechanistic studies of the apoptotic effects induced by Mito-EP-**3b**

It has been reported that a change of $\Delta\psi_m$ triggers cytochrome c release and subsequently apoptosis through caspase-9 activation. To confirm that the observed apoptotic effects in MCF-7 cells by Mito-EP-**3b** were exerted via the mitochondrial pathway, we measured the expression levels of cytochrome c, caspase-9, cleaved caspase-9, caspase-7, cleaved caspase-7, Bax and Bcl-2 using Western blotting. As shown in Figure 7, the content of cytochrom c in the cytoplasm increased; meanwhile cytochrome c triggered the activation of caspase-9 and caspase-7. Accordingly, as the end point of the signaling pathway, after treatment with Mito-EP-**3b**, the expression of Bax began to increase, while Bcl-2 expression was significantly suppressed. These effects were all achieved in a dose-dependent manner. The above results illustrate that Mito-EP-**3b** was able to induce the mitochondrial pathway of apoptosis in MCF-7 cells.

Conclusions

In the development of effective anticancer agents, mitochondria are acknowledged to be an important drug target. The triphenylphosphonium-based modification of drugs to facilitate mitochondrial targeting is an effective approach, as there is a wealth of literature on the good biological effects of small molecules containing TPP. Ergosterol peroxide (EP, **1**) was isolated from the traditional Chinese medicine *Ganoderma lucidum* in our previous study. During our extensive screening for natural antitumor agents, EP showed moderate antitumor activities. Thus, to discover mitochondrion-targeting antitumor agents, and the corresponding EP mitochondrion-targeted derivatives (Mito-EP-**3a-3d**) were synthesized through conjugation EP with the TTP moiety via alkyl linker.

In vitro cytotoxic effects of these Mito-EP derivatives towards human HepG2, MCF-7 and HeLa cells were evaluated using MTT assay. They all exhibited significant cytotoxic activity. The most potent compound, Mito-EP-**3b**, was 9.7-fold more efficacious than EP in the MCF-7 cell line (IC_{50} = 2.04 μM) and showed good selectivity (SI = IC_{50}GES-1/IC_{50}MCF-7 = 4.04). SAR analysis proved that the length of the carbon chain was able to influence the cytotoxic effects of all these derivatives. Mito-EP-**3b** in a linker with four carbons displayed better biological abilities than the other three derivatives. To further investigate the antitumor mechanism of Mito-EP-**3b**, additional pharmacological experiments were performed *in vitro*.

Mitochondrion-targeted antitumor agents can trigger mitochondrial dysfunction via different mechanisms, such as mitochondrial apoptotic pathway, leading to cancer cell death. It is known that the mitochondrial apoptotic pathway is related to the decrease in mitochondrial membrane potential and excessive production of ROS, as well as the release of

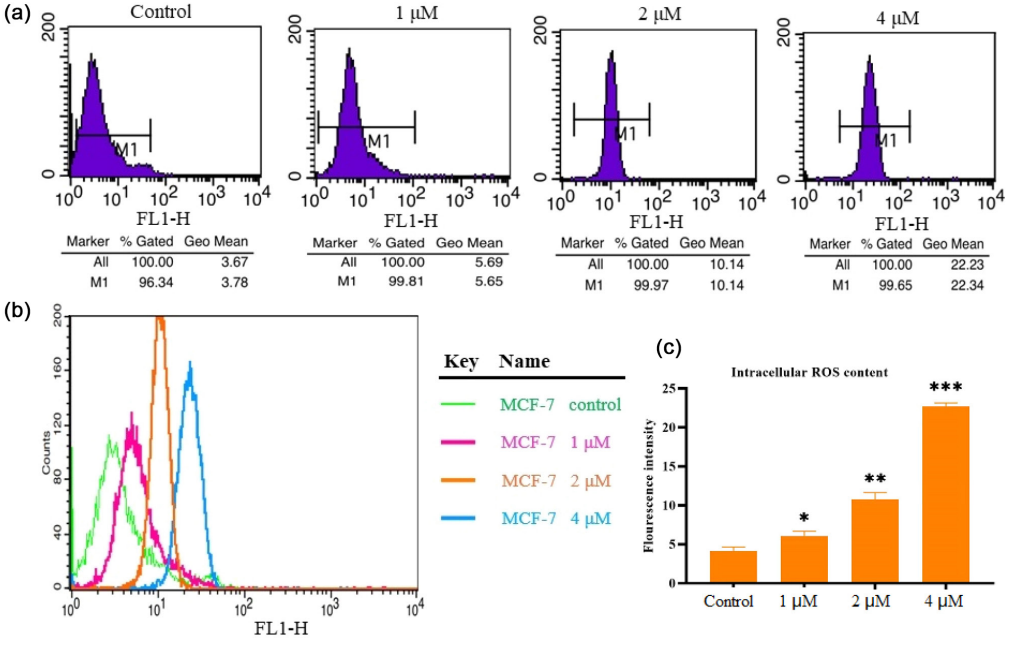

Figure 6. The effect of Mito-EP-**3b** on intracellular ROS in MCF-7 cells was determined by flow cytometry. (a) MCF-7 cells were treated with Mito-EP-**3b** for 48 h and stained with DCFH-DA and then analyzed by flow cytometry. (b) The histograms were merged together. (c) The bar graph represents the intracellular ROS level at different concentrations of Mito-EP-**3b**. Data are represented as average ± SD (n = 3). *$P < 0.05$, **$P < 0.01$, ***$P < 0.001$.

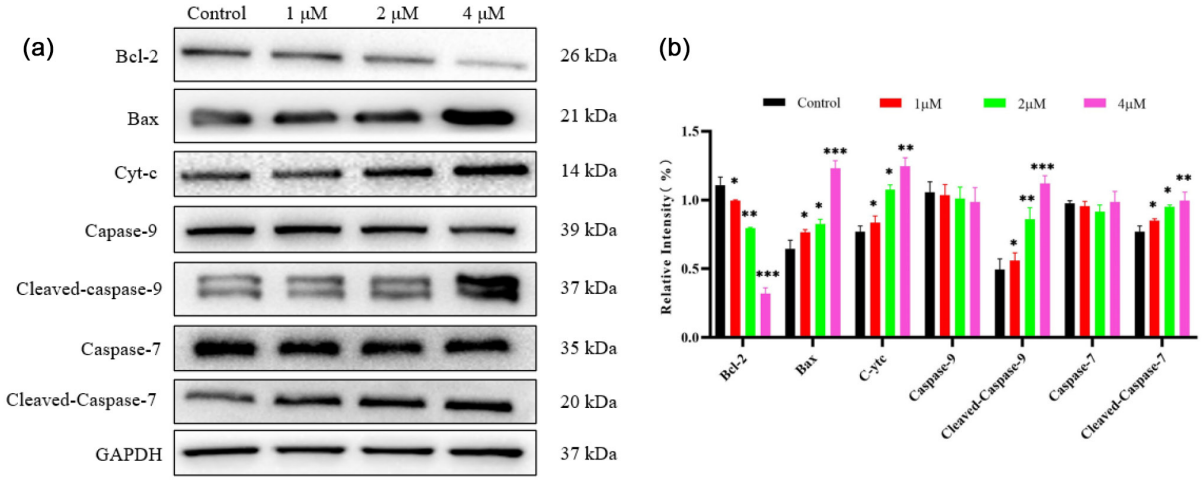

Figure 7. Effects of Mito-EP-**3b** on the expression of apoptosis-related proteins. (a) MCF-7 cells were treated with Mito-EP-**3b** for 48 h at gradient concentrations (0, 1, 2 and 4 μM). The expression of cyt-c, capase-9, cleaved capase-9, capase-7, cleaved capase-7, Bax, and Bcl-2 were analyzed by Western blotting using the corresponding specific antibodies. (b) Quantitative analysis of the related protein expression. Data are represented as average ± SD (n = 3). *$P < 0.05$; **$P < 0.01$, ***$P < 0.001$.

cytochrome c and other cofactors from the mitochondria, inducing subsequent caspase activation regulated by Bcl-2 family proteins. Our subsequent preliminary mechanistic investigation demonstrated that Mito-EP-**3b** exerts significant cytotoxic effects by inducing MCF-7 cells early apoptosis. Furthermore, Mito-EP-**3b** was found to reduce mitochondrial membrane potential, and induce ROS production. Additionally, the level of apoptosis-related protein expression was assessed. As a result, Mito-EP-**3b** up-regulated the expression of cytochrome c, Bax, cleaved caspase-9 and cleaved caspase-7, and down-regulated the expression of Bcl-2. These findings demonstrated that Mito-EP-**3b** could induce MCF-7 cell apoptosis by triggering the mitochondrial apoptotic pathway. The above findings incentivize the further study of Mito-EP-**3b** derivative as potent anticancer agent.

Supplementary Information

Supplementary file (containing the NMR and HRMS charts for the synthesized compounds) is available free of charge at https://jbcs.sbq.org.br as PDF file.

Acknowledgments

We gratefully acknowledge the financial support by Project of Qiqihar Science and Technology Bureau (LHYD-2021005).

Author Contributions

Ming Bu and Yu Lin were responsible for conceptualization; Wenkang Ren, Jiafeng Wang and Jiale Wu for methodology and chemistry experiments; Yinglong Han, Haijun Wang and Wenkang Ren for biology experiments; Jiafeng Wang and Yu Lin for writing original draft; Ming Bu for writing-review and editing.

References

1. Sung, H.; Ferlay, J.; Siegel, R. L.; Laversanne, M.; Soerjomataram, I.; Jemal, A.; Bray, F.; *CA-Cancer J. Clin.* **2021**, *71*, 209. [Crossref]
2. Goodman, J. E.; Mayfield, D. B.; Becker, R. A.; Hartigan, S. B.; Erraguntla, N. K.; *Regul. Toxicol. Pharmacol.* **2020**, *113*, 104639. [Crossref]
3. Dolgin, E.; *Nat Cancer*. **2021**, *2*, 1248. [Crossref]
4. Deng, L.; Feng, Z.; Deng, H.; Jiang, Y.; Song, K.; Shi, Y.; Liu, S.; Zhang, J.; Bai, S.; Qin, Z.; Dong, A.; *ACS Appl. Mater. Interfaces* **2019**, *11*, 31743. [Crossref]
5. Amin, S. A.; Adhikari, N.; Jha, T.; Gayen, S.; *Anticancer Agents Med. Chem*. **2018**, *18*, 1796. [Crossref]
6. Newman, D. J.; Cragg, G. M.; *J. Nat. Prod*. **2020**, *83*, 770. [Crossref]
7. Bu, M.; Yang, B. B.; Hu, L.; *Curr. Med. Chem*. **2016**, *23*, 383. [Crossref]
8. Sun, X.; Yan, P.; Zou, C.; Wong, Y. K.; Shu, Y.; Lee, Y. M.; Zhang, C.; Yang, N. D.; Wang, J.; Zhang, J.; *Med. Res. Rev*. **2019**, *39*, 2172. [Crossref]
9. Ueoka, R.; Nakao, Y.; Kawatsu, S.; Yaegashi, J.; Matsumoto, Y.; Matsunaga, S.; Furihata, K.; van Soest, R. W.; Fusetani, N.; *J. Org. Chem*. **2009**, *74*, 4203. [Crossref]
10. He, F.; Pu, J.-X.; Huang, S.-X.; Wang, Y.-Y.; Xiao, W.-L.; Li, L.-M.; Liu, J.-P.; Zhang, H.-B.; Li, Y.; Sun, H.-D.; *Org. Lett.* **2010**, *12*, 1208. [Crossref]
11. Li, H.; Huang, H.; Shao, C.; Huang, H.; Jiang, J.; Zhu, X.; Liu, Y.; Liu, L.; Lu, Y.; Li, M.; Lin, Y.; She, Z.; *J. Nat. Prod*. **2011**, *74*, 1230. [Crossref]

12. Li, X.; Ba, Q.; Liu, Y.; Yue, Q.; Chen, P.; Li, J.; Zhang, H.; Ying, H.; Ding, Q.; Song, H.; Liu, H.; Zhang, R.; Wang, H.; *Cell. Discovery* **2017**, *3*, 17042. [Crossref]
13. Sharma, V.; Chaudhry, A.; Chashoo, G.; Arora, R.; Arora, S.; Saxena, A. K.; Ishar, M. P. S.; *Eur. J. Med. Chem*. **2014**, *87*, 228. [Crossref]
14. Schirmeister, T.; Oli, S.; Wu, H.; Della Sala, G.; Costantino, V.; Seo, E. J.; Efferth, T.; *Mar. Drugs* **2017**, *15*, 63. [Crossref]
15. Cabrera-Afonso, M. J.; Lucena, S. R.; Juarranz, Á.; Urbano, A.; Carreño, M. C.; *Org. Lett*. **2018**, *20*, 6094. [Crossref]
16. Wu, Q.-P.; Xie, Y.-Z.; Deng, Z.; Li, X. M.; Yang, W.; Jiao, C. W.; Fang, L.; Li, S. Z.; Pan, H. H.; Yee, A. J.; Lee, D. Y.; Li, C.; Zhang, Z.; Guo, J.; Yang, B. B.; *PLoS One* **2012**, *7*, e44579. [Crossref]
17. Li, X. M.; Wu, Q. P.; Bu, M.; Hu, L. M.; Du, W. W.; Jiao, C. W.; Pan, H. H.; Sdiri, M.; Wu, N.; Xie, Y. Z.; Yang, B. B.; *Oncotarget* **2016**, *7*, 33948. [Crossref]
18. Tan, W.; Pan, M.; Liu, H.; Tian, H.; Ye, Q.; Liu, H.; *OncoTargets Ther.* **2017**, *10*, 3467. [Crossref]
19. Yang, Y.; Luo, X.; Yasheng, M.; Zhao, J.; Li, J.; Li, J.; *Food Funct*. **2020**, *11*, 4171. [Crossref]
20. Nowak, R.; Drozd, M.; Mendyk, E.; Lemieszek, M.; Krakowiak, O.; Kisiel, W.; Rzeski, W.; Szewczyk, K.; *Molecules* **2016**, *21*, 946. [Crossref]
21. Yodsing, N.; Lekphrom, R.; Sangsopha, W.; Aimi, T.; Boonlue, S.; *Curr. Microbiol*. **2018**, *75*, 513. [Crossref]
22. Chen, Z. G.; Bishop, K. S.; Tanambell, H.; Buchanan, P.; Smith, C.; Quek, S. Y.; *Food Funct*. **2019**, *10*, 6633. [Crossref]
23. Govindharaj, M.; Arumugam, S.; Nirmala, G.; Bharadwaj, M.; Murugiyan, K.; *J. Fungi* **2019**, *5*, 16. [Crossref]
24. Bu, M.; Cao, T. T.; Li, H. X.; Guo, M. Z.; Yang, B. B.; Zhou, Y.; Zhang, N.; Zeng, C. C.; Hu, L. M.; *Steroids* **2017**, *124*, 46. [Crossref]
25. Bu, M.; Cao, T. T.; Li, H. X.; Guo, M. Z.; Yang, B. B.; Zeng, C. C.; Hu, L. M.; *ChemMedChem* **2017**, *12*, 466. [Crossref]
26. Bu, M.; Li, H.; Wang, H.; Wang, J.; Lin, Y.; Ma, Y.; *Molecules* **2019**, *24*, 3307. [Crossref]
27. Bu, M.; Cao, T.; Li, H.; Guo, M.; Yang, B. B.; Zeng, C.; Zhou, Y.; Zhang, N.; Hu, L.; *Bioorg. Med. Chem. Lett.* **2017**, *27*, 3856. [Crossref]
28. Wang, H. J.; Bu, M.; Wang, J.; Liu, L.; Zhang, S.; *Russ. J. Bioorg. Chem*. **2019**, *45*, 585. [Crossref]
29. Li, H. L.; Wang, H. J.; Wang, J.; Lin, Y.; Ma, Y.; Bu, M.; *Steroids* **2020**, *153*, 108471. [Crossref]
30. Wheeler, H. E.; Maitland, M. L.; Dolan, M. E.; Cox, N. J.; Ratain, M. J.; *Nat. Rev. Genet*. **2013**, *14*, 23. [Crossref]
31. Bernardi, P.; Scorrano, L.; Colonna, R.; Petronilli, V.; Di Lisa, F.; *Eur. J. Biochem*. **1999**, *264*, 687. [Crossref]
32. Tait, S. W.; Green, D. R.; *J. Cell Sci*. **2012**, *125*, 807. [Crossref]
33. Fulda, S.; Galluzzi, L.; Kroemer, G.; *Nat. Rev. Drug. Discovery* **2010**, *9*, 447. [Crossref]
34. Yan, B.; Dong, L.; Neuzil, J.; *Mitochondrion* **2016**, *26*, 86. [Crossref]
35. Gogvadze, V.; Orrenius, S.; Zhivotovsky, B.; *Trends Cell Biol*. **2008**, *18*, 165. [Crossref]
36. D'Souza, G. G.; Wagle, M. A.; Saxena, V.; Shah, A.; *Biochim. Biophys. Acta* **2011**, *1807*, 689. [Crossref]
37. Shi, X.; Zhang, T.; Lou, H.; Song, H.; Li, C.; Fan, P.; *J. Med. Chem*. **2020**, *63*, 11786. [Crossref]
38. Smith, R. A.; Porteous, C. M.; Gane, A. M.; Murphy, M. P.; *Proc. Natl. Acad. Sci. U. S. A*. **2003**, *100*, 5407. [Crossref]
39. Yilmaz, V. T.; Icsel, C.; Batur, J.; Aydinlik, S.; Cengiz, M.; Buyukgungor, O.; *Dalton Trans*. **2017**, *46*, 8110. [Crossref]
40. Tsepaeva, O. V.; Nemtarev, A. V.; Abdullin, T. I.; Grigor'eva, L. R.; Kuznetsova, E. V.; Akhmadishina, R. A.; Ziganshina, L. E.; Cong, H. H.; Mironov, V. F.; *J. Nat. Prod.* **2017**, *80*, 2232. [Crossref]
41. Grymel, M.; Zawojak, M.; Adamek, J.; *J. Nat. Prod.* **2019**, *82*, 1719. [Crossref]
42. Chen, W.; Hu, S.; Mao, S.; Xu, Y.; Guo, H.; Li, H.; Paulsen, M. T.; Chen, X.; Ljungman, M.; Neamati, N.; *ChemMedChem* **2020**, *15*, 2029. [Crossref]
43. Zhao, L.; Duan, X.; Cao, W.; Ren, X.; Ren, G.; Liu, P.; Chen, J.; *Foods* **2021**, *10*, 2470. [Crossref]
44. Jin, L.; Dai, L.; Ji, M.; Wang, H.; *Bioorg. Chem*. **2019**, *85*, 179. [Crossref]
45. Xu, C.; Xiao, L.; Zhang, X.; Zhuang, T.; Mu, L.; Yang, X.; *Med. Chem. Lett*. **2021**, *39*, 127912. [Crossref]
46. Zhang, C. J.; Wang, J.; Zhang, J.; Lee, Y. M.; Feng, G.; Lim, T. K.; Shen, H. M.; Lin, Q.; Liu, B.; *Angew. Chem., Int. Ed.* **2016**, *55*, 13770. [Crossref]
47. Song, H.; Xing, W.; Shi, X.; Zhang, T.; Lou, H.; Fan, P.; *Bioorg. Med. Chem*. **2021**, *50*, 116466. [Crossref]
48. Zielonka, J.; Joseph, J.; Sikora, A.; Hardy, M.; Ouari, O.; Vasquez-Vivar, J.; Cheng, G.; Lopez, M.; Kalyanaraman, B.; *Chem. Rev*. **2017**, *117*, 10043. [Crossref]
49. Ju, W.; Li, N.; Wang, J.; Yu, N.; Lei, Z.; Zhang, L.; Sun, J.; Chen, L.; *Bioorg. Chem*. **2021**, *115*, 105249. [Crossref]
50. Ye, Y.; Zhang, T.; Yuan, H.; Li, D.; Lou, H.; Fan, P.; *J. Med. Chem*. **2017**, *60*, 6353. [Crossref]
51. *IBM SPSS Statistics* 24.0; SPSS Inc., Chicago, IL, USA, 2016.

Submitted: January 25, 2023
Published online: April 17, 2023